Int. J. Solids Structures, 1968, Vol. 4, pp. 197 to 223. Pergamon Press. Printed in Great Britain

EXPERIMENTAL DATA ON SMALL-PLASTIC DEFORMATION WAVES IN ANNEALED ALUMINUM

O. W. DILLON, JR.

University of Kentucky, Lexington, Kentucky

Abstract—Experimental data on the propagation of deformation waves in annealed aluminum tubes and rods in which the maximum axial strain is between 100 μin/in and 3000 μin/in are reported. A large variation in propagation speed is observed between specimens which are thought to be identical. The variation is real and is relatively larger near yielding than it is at higher values of strain. Strain histories from a number of specimens are therefore averaged to provide meaningful data for possible comparison with theoretical results. The standard deviation in the data used to obtain the propagation speed is also included. It is shown that in the averaged history, strains above 500 μin/in propagate at constant speed and therefore are as consistent with a strain-rate independent theory as with any other. In the averaged history strains below 300 μin/in have a speed of propagation which decreases as the wave travels down the bar and therefore indicate an apparent strain-rate effect. This apparent strain-rate effect may either be real or that of a mechanically unstable material. Data which strongly suggests that the unstable material is more generally applicable is presented.

INTRODUCTION

THE case of the propagation of a uniaxial stress state into an undeformed portion of a medium at rest is a basic one in the mechanics of continua. In particular, when the stress exceeds the elastic limit, one would like experimental results obtained during this test to serve as a basis for the general material response function. However in this range of the response, there is no clearly understood (i.e. generally accepted) viewpoint on how to perform experiments and to interpret the results. For example, the importance of "strain-rates" in the constitutive equation is not yet firmly established for common metals. The proceedings of a recent colloquium [1] illustrate the current state of the art.

This paper makes a somewhat different point by reporting the results of tests on several specimens which are believed to have been identically prepared. It will be shown that the variation in the propagation speed between specimens, is large and that this is inherent in the material response. Hence the author concludes that one can use *any* theory of wave propagation and material description which has gross agreement with the experimental data. The theory which he would "prefer" is chosen on grounds of simplicity or agreement with tests of other types (i.e. static) but not on the basis of slightly better agreement with data from a small number of wave experiments. Thus, except possibly near yielding, the author "prefers" the Karman–Taylor Rakhmatulin strain-rate independent theory as modified by the unstable material concept [2–4] to include the observed incremental wave response. This result, but stated differently, was reached by Bell [5, 6] some years ago for aluminum annealed in the same way as that used in the present experiments. In contrast with [5, 6], we use wire resistance strain gauges, concentrate on the region near the yield point, make measurements on a single specimen at several axial locations and use very simple experimental apparatus which can be easily reproduced by other interested investigators. It is hoped that these independent measurements will establish that the work in [5, 6] is exceptionally sound and that there exists at least one material (annealed

aluminum) for which the strain-rate independent theory is as adequate as any other. Additional new data which is consistent with the unstable concept [2–4] but not with the smooth stress–strain relation is also presented.

The large variation of the propagation speed in certain regions of response is the focus of this paper. The only other example known to the author where statistical data on plastic waves is the dominant theme is for the case of lead [12].

TECHNIQUE

Material

The commercially pure aluminum (1100 alloy) which is used here is annealed at 1100°F and furnace cooled; this results in a fine grained structure and makes it the same material as that used in our previous studies [2–4]. It is also nominally the same in composition and is annealed the same way in another [5, 6] series of basic studies of plastic wave propagation. In view of the variation in dynamic response to be presented, it is emphasized that the static data also has variations in it as previously reported [3, 7, 8]. Other data on annealed aluminum, but of (possibly) different details of composition and heat treatment, are contained in [9, 10].

The standard specimen used here is 36 in. long and is a 0·50 in. o.d. by 0·375 in. i.d. tube, but other lengths and a few 0·25 in. dia. rods are also tested as indicated in the text. Care is used in selecting specimens which are initially straight.

Impact tester

A predominantly axial deformation is produced by impacting the end of the specimen with a steel plunger which is propelled by releasing a compressed spring. The specimen is hung from an A frame by two long (36 in.) thin strings. After the specimen is impacted it flies a short distance where it hits a buffer and is then caught by the operator. In the meantime the desired data has been obtained. Positioning devices are used to align the specimen and plunger for each hit. As described below some small bending still exists; but this can be detected, and if desired the results of that specimen ignored.

It is a merit of the present system that it is simple and one that can readily be duplicated. So far this has not happened for the method used in [5] which however is far more elegant and has certain other obvious advantages for some types of information. A schematic of the present system is shown in Fig. 1.

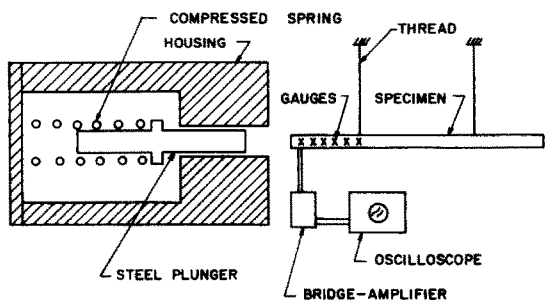

FIG. 1. A schematic of the system used to produce an impact type loading.

Strain measurement

The strain time histories at four to six axial positions on each specimen are measured by displaying the output of SR-4-A-8 wire resistance gauges on an oscilloscope. The gauges are attached to the specimen by means of Post-Yield Cement and are usually spaced at two inch intervals along the bar. The change in resistance of the gauge is made into a suitable oscilloscope signal by using an Ellis Associates Model BAM-1 Bridge Amplifier. The oscilloscope uses a Tektronix Type A-74 (four channel) plug-in unit which splits a single electron beam into four traces. The gauges are connected to the Ellis Associates Amplifier using very fine copper wire in order to reduce bending during the motion of the specimen.

Because the strain histories do not change drastically with distance, the system employed gives good *comparison* data for the several axial stations especially when they are not near the impact face. There will be some unloading and (possibly) contributions from reflections in the plunger. Furthermore there is an impedance mismatch between the plunger and specimen. However since strain histories at different positions are compared, these are irrelevant. Said differently, we compare strain histories (away from the ends) and deliberately do not attempt to correlate boundary conditions with internal response.

EXPERIMENTAL DATA

Elastic region

The accuracy of the apparatus described above is established by the results of tests made in the elastic range of the material response. A typical strain history*, for the elastic region is shown in Fig. 2 where the existence of deviations from the elementary bar theory

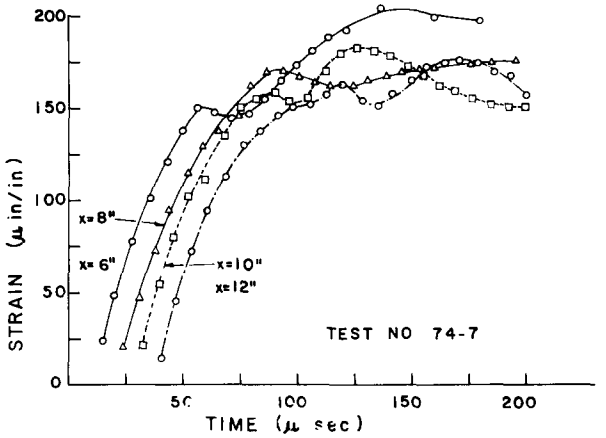

FIG. 2. Typical 0·50 in. tubular specimen strain histories at several axial stations when the material remains elastic.

is evident near 150 μin/in of strain. The time required for a given level of strain to propagate between $\chi = 4{\cdot}0$ in. and $\chi = 10{\cdot}0$ in. has been measured for several tests. The average value of these time increments and the standard deviation for these quantities are shown in Table 1. The average of the time required for a wave to travel six inches is 26·3 μsec. Thus the average value of the propagation speed is $2{\cdot}3 \times 10^5$ in/sec which is (approximately) equal to the bar velocity† given by the square root of Young's modulus E, divided by the mass density, ρ.

* Figure 2, is for a specimen previously deformed into the plastic range.

† The bar velocity is $2{\cdot}02 \times 10^5$ in/sec for aluminum. See also Table 5, where this value is actually observed.

TABLE 1. THE TIME INTERVAL, Δt, FOR A GIVEN VALUE OF STRAIN, ε, TO PROPAGATE BETWEEN $\chi = 4$ in. AND $\chi = 10$ in. THE NUMBER OF SPECIMENS AND THE STANDARD DEVIATION OF THE TIME INTERVAL ARE DESIGNATED AS n AND S.D. RESPECTIVELY AND THE SPECIMENS REMAIN ELASTIC

ε (μin/in)	Δt (μ sec)	n	S.D. (μ sec)
17·0	26·4	10	1·5
34·0	26·6	11	1·7
51·0	26·0	11	1·9
68·0	25·4	10	2.2
85·0	25·7	11	2·4
102·0	26·8	10	3·3
Average	26·3		

The results for a series of specimens different than the ones used in obtaining data for Table 1 are given in Table 2 and the averaged response shown in Fig. 3. There are deviations from the elementary bar response that are most dramatic between $\chi = 6{\cdot}0$ in. and $\chi = 8{\cdot}0$ in. In some tests the strain histories of points at 6·0 and 8·0 inches actually cross near 105 μin/in. This is consistent with the larger standard deviation for higher values of the strain. For the same strains used in Table 1 the average time increment in Table 2 is 26·2 μsec, illustrating adequate reproductibility of the averaged data.

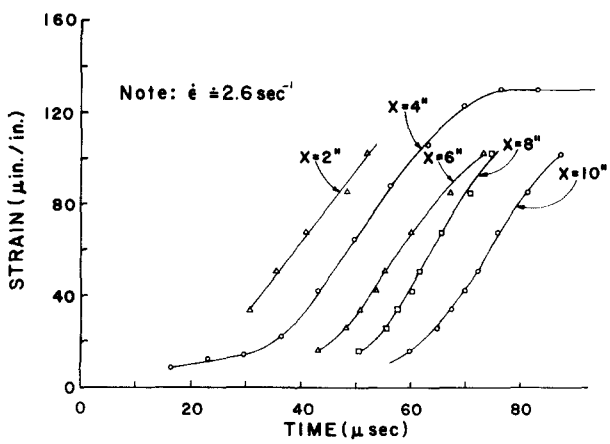

FIG. 3. "Averaged" 0·50 in. tubular specimen strain histories at several axial positions when the material is elastic.

In practice these elastic impacts are very valuable because they permit the checking of the apparatus and thereby add greatly to the reduction of bending strains and to verifying calibration factors for the gauges and amplifier. Since the standard deviation in the overall measurements (Table 1) is less than 3 μsec, and the data for smaller intervals also has less than this value; we conclude that the inherent system error is certainly no larger than 3 μsec.

TABLE 2. THE TIME INTERVAL, Δt, FOR A GIVEN VALUE OF STRAIN, ε, TO PROPAGATE BETWEEN THE DESIGNATED AXIAL LOCATIONS. THE NUMBER OF SPECIMENS, n, AND THE STANDARD DEVIATION OF THE TIME INTERVAL, S.D., ARE ALSO SHOWN. ALL SPECIMENS REMAIN ELASTIC IN THESE TESTS AND ARE DIFFERENT ONES THAN USED IN TABLE 1

	$\chi = 2$–$\chi = 4$	$\chi = 4$–$\chi = 6$	$\chi = 6$–$\chi = 8$	$\chi = 8$–$\chi = 10$
		$\varepsilon = 8{\cdot}5$ μin/in		
Δt (μ sec)	—	—	8·7	8·3
n	—	—	7	7
S.D. (μ sec)	—	—	2·6	1·3
		$\varepsilon = 17{\cdot}0$ μin/in		
Δt (μ sec)	—	9·8	7·7	9·0
n	—	11	7	7
S.D. (μ sec)	—	3·6	2·5	0·90
		$\varepsilon = 25{\cdot}5$ μin/in		
Δt (μ sec)	—	10·1	7·4	9·3
n	—	7	7	7
S.D. (μ sec)	—	2·5	2·6	0·5
		$\varepsilon = 34{\cdot}0$ μin/in		
Δt (μ sec)	10·4	9·8	7·1	9·6
n	2	12	7	7
S.D. (μ sec)	—	3·2	3·1	0·9
		$\varepsilon = 42{\cdot}5$ μin/in		
Δt (μ sec)	—	10·6	6·7	9·8
n	—	7	7	7
S.D. (μ sec)	—	3·4	3·2	0·9
		$\varepsilon = 51{\cdot}0$ μin/in		
Δt (μ sec)	10·2	9·7	6·6	9·7
n	3	12	7	7
S.D. (μ sec)	1·7	3·9	3·2	1·1
		$\varepsilon = 68{\cdot}0$ μin/in		
Δt (μ sec)	9·7	9·4	5·4	10·2
n	3	11	7	7
S.D. (μ sec)	—	3·2	4·6	1·7
		$\varepsilon = 85{\cdot}0$ μin/in		
Δt (μ sec)	7·2	12·0	3·6	10·4
n	3	10	8	8
S.D. (μ sec)	—	2·1	6·7	2·3
		$\varepsilon = 102{\cdot}0$ μin/in		
Δt (μ sec)	9·1	12·6	1·1	12·6
n	1	9	8	8
S.D. (μ sec)	—	10·1	8·8	4·7

However one does not have a perfect example of the elementary bar. To provide partial knowledge of the deviations from the one dimensional stress that is assumed in bar theory, rosette gauges were used in some specimens to measure both hoop and axial strains. These results are presented below.

TABLE 3. THE TIME INTERVAL, Δt, FOR A GIVEN VALUE OF STRAIN, ε, TO PROPAGATE BETWEEN THE DESIGNATED AXIAL STATIONS IN 0·50-in. TUBULAR SPECIMENS OF ANNEALED ALUMINUM. THE NUMBER OF SPECIMENS, n; THE STANDARD DEVIATION, S.D.; THE MAXIMUM POSITIVE AND NEGATIVE DEVIATIONS IN THE TIME INTERVAL ARE ALSO GIVEN. THIS DATA IS FOR THE IMPACT WHICH PRODUCES INITIAL PLASTIC DEFORMATION

	$\chi = 2$–$\chi = 4$	$\chi = 4$–$\chi = 6$	$\chi = 6$–$\chi = 8$	$\chi = 8$–$\chi = 10$	$\chi = 10$–$\chi = 12$
			$\varepsilon = 85$ μin/in		
Δt (μ sec)	8·5	10·0	6·8	8·8	10·8
n	6	23	14	16	9
S.D. (μ sec)	2·3	3·1	3·4	2·7	5·2
max. pos. dev. (μ sec)	4·0	8·3	4·4	7·7	7·7
max. neg. dev. (μ sec)	1·9	4·2	7·2	2·2	8·0
			$\varepsilon = 131$ μin/in		
Δt (μ sec)	11·1	10·9	8·0	8·8*	12·5*
n	6	27	20	17	10
S.D. (μ sec)	4·0	4·0	5·9	3·6	7·3
max. pos. dev. (μ sec)	5·6	25·0	21·0	9·7	15·7
max. neg. dev. (μ sec)	5·2	7·0	6·8	3·7	9·5
			$\varepsilon = 170$ μin/in		
Δt (μ sec)	12·5	13·0	12·6	14·8*	20·5*
n	6	26	20	18	10
S.D. (μ sec)	6·7	5·7	15·8	13·8	20·4
max. pos. dev. (μ sec)	8·3	9·2	57·4	27·4	46·0
max. neg. dev. (μ sec)	8·3	9·3	12·6	10·8	10·40
			$\varepsilon = 213$ μin/in		
Δt (μ sec)	16·0	19·2	14·8	25·6*	31·5*
n	6	25	18	16	7
S.D. (μ sec)	5·6	10·8	13·7	16·8	20·3
max. pos. dev. (μ sec)	7·3	34·4	19·3	37·6	35·2
max. neg. dev. (μ sec)	9·4	19·3	10·3	17·7	22·4
			$\varepsilon = 255$ μin/in		
Δt (μ sec)	20·0	24·6	30·5	33·2	40·0
n	6	23	19	13	6
S.D. (μ sec)	6·7	10·1	21·5	16·3	22·5
max. pos. dev. (μ sec)	9·2	36·2	46·3	22·0	25·9
max. neg. dev. (μ sec)	7·5	24·6	26·2	27·5	33·4
			$\varepsilon = 298$ μin/in		
Δt (μ sec)	22·2	29·4	25·5	33·6	45·6
n	5	20	15	12	5
S.D. (μ sec)	5·6	12·9	12·9	13·1	23·2
max. pos. dev. (μ sec)	9·5	47·4	32·8	24·8	36·0
max. neg. dev. (μ sec)	4·7	22·8	23·2	17·8	27·2
			$\varepsilon = 340$ μin/in		
Δt (μ sec)	25·0	32·0	34·9	38·5	39·0
n	5	18	15	11	4
S.D. (μ sec)	4·4	9·2	15·5	10·5	13·5
max. pos. dev. (μ sec)	8·3	18·0	36·7	17·3	17·7
max. neg. dev. (μ sec)	4·2	19·5	24·2	24·4	13·9

* Does not include data where specimen is elastic at these positions, i.e. like Fig. 17.

Table 3 (contd.)

	$\chi = 2$–$\chi = 4$	$\chi = 4$–$\chi = 6$	$\chi = 6$–$\chi = 8$	$\chi = 8$–$\chi = 10$	$\chi = 10$–$\chi = 12$
			$\varepsilon = 425\ \mu$in/in		
Δt (μ sec)	29·3	38·4	33·1	40·2	—
n	5	15	10	9	—
S.D. (μ sec)	4·6	10·3	8·0	11·4	—
max. pos. dev. (μ sec)	6·5	22·1	90·0	15·0	—
max. neg. dev. (μ sec)	3·5	15·4	20·0	40·2	—
			$\varepsilon = 510\ \mu$in/in		
Δt (μ sec)	33·3	40·6	31·7	—	—
n	5	12	8	—	—
S.D. (μ sec)	4·6	9·7	8·6	—	—
max. pos. dev. (μ sec)	8·3	21·8	15·8	—	—
max. neg. dev. (μ sec)	5·0	15·5	15·0	—	—

Initial plastic hit

After the specimen has been subjected to several small impacts which produce elastic strains, the spring is further compressed to provide a stress large enough to cause permanent straining of the material. Typical experimental records for these first plastic hits are shown in Figs. 4–6. Figures 4 and 5 illustrate the variety of responses which are obtained. For example in Fig. 4 the apparent yield strain is 210 μin/in, but in Fig. 5 it is only 160 μin/in. This variation in the yield strain for different specimens which are thought to be identical is the source of much of the real variation of propagation speeds reported in this paper. In order to examine whether the strain-rate was a prominent factor in the variation in the yield strain, the plunger spring was initially compressed more than it was when obtaining data for Figs. 4 and 5. The results are presented in Fig. 6. The larger spring force resulted in an increase in strain-rate from 2·5 μin/in/μsec in Fig. 5 to 10 μin/in/μsec in Fig. 6 but to within experimental accuracy the yield strain in both of these tests is the same.

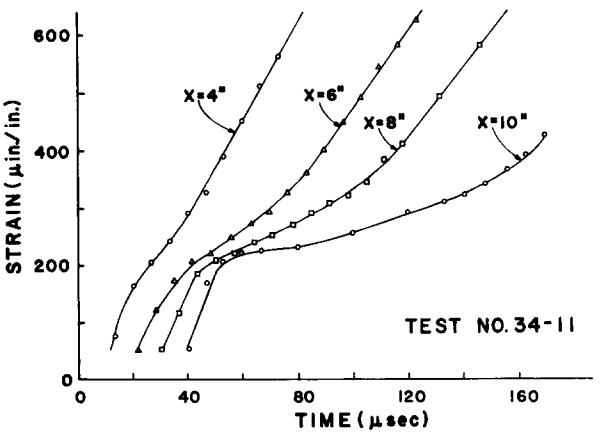

FIG. 4. Typical strain histories at several axial positions at a small initial plastic impact of tubes. The residual strains are (approximately): 610, 610, 465, and 240 μin/in at $\chi = 4$, 6, 8 and 10 in. respectively.

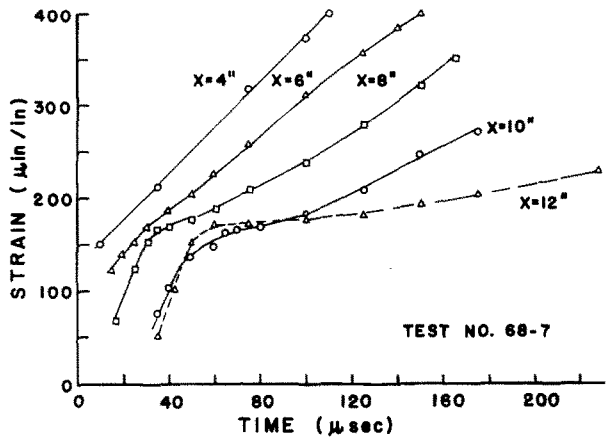

FIG. 5. Typical tubular specimen strain histories at several axial positions for small initial plastic impact. The residual strains are (approximately): 365, 340, 270, 240 and 50 μin/in at $\chi = 4$, 6, 8, 10, and 12 in. respectively.

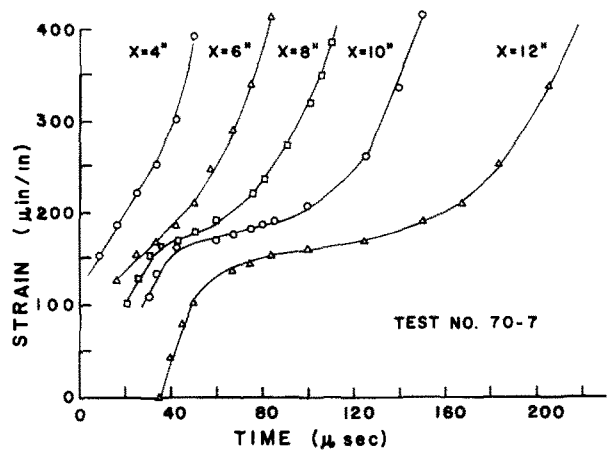

FIG. 6. Typical tubular specimen strain histories at several axial positions for a large initial plastic impact in order to produce higher strain rates. The approximate permanent strains are: 1620, 1550, 1570, 1410 and 1020 μin/in at $\chi = 4$, 6, 8, 10 and 12 in. respectively.

Data of the type shown in Figs. 4–6 provide the time increments for a given value of strain to propagate between gauge positions. Such data has considerable (relative) variation in it. Hence the response of a number of specimens must be averaged to provide meaningful data. The summary of such average results for the small initial impacts and their variations are shown in Figs. 7–10 and in Table 3. Figure 7 is the averaged time histories at each of the indicated stations for a series of tubes, while similar data on a small series of rods is shown in Fig. 8 and Table 4. A comparison of the data given in Figs. 7 and 8 for tubes and rods, shows that there is excellent agreement between the responses for distances between $\chi = 2{\cdot}0$–$\chi = 6{\cdot}0$ in. However the wave slows down somewhat nearer the impact face in the case of the rods. Table 4 makes this slowing down a little easier to see.

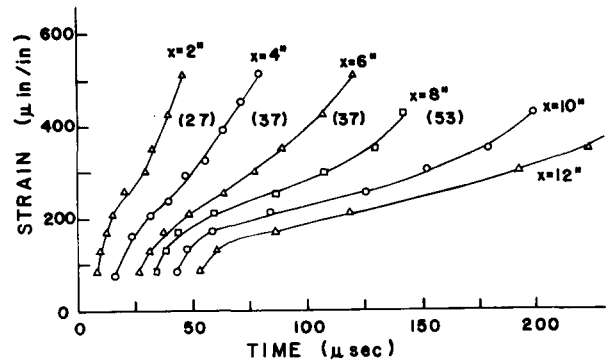

FIG. 7. "Averaged" strain histories at several axial positions for 0·50 in. o.d. tubular specimens subjected to (relatively) small initial plastic impacts.

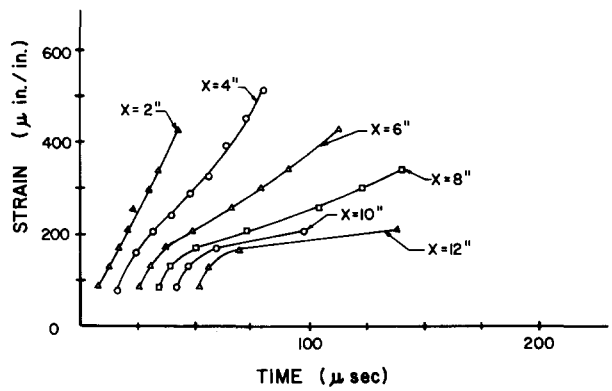

FIG. 8. "Averaged" strain histories at several axial positions for 0·25 in. *rods* subjected to relatively small plastic impacts.

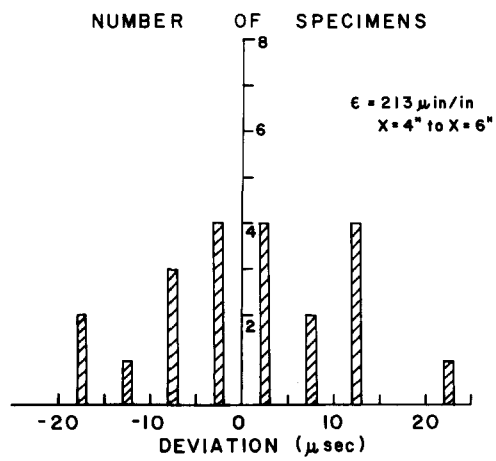

FIG. 9. The distribution of experimental values of the time required for a strain of 213 μin/in to propagate between $\chi = 4$ in. and $\chi = 6$ in. The number of specimens having a time interval which deviates from the average value of 19·2 μsec is given for 5 μsec intervals. All specimens are 0·50 in. o.d. tubes being subjected to stresses which are here producing the first plastic strains since being annealed.

TABLE 4. THE TIME INTERVAL, Δt, FOR A GIVEN VALUE OF STRAIN, ε, TO PROPAGATE BETWEEN THE DESIGNATED AXIAL STATIONS IN 0·25 in. dia. ANNEALED ALUMINUM RODS. THE STANDARD DEVIATION OF THE TIME INTERVAL, S.D., AND NUMBER OF SPECIMENS, n, ARE ALSO GIVEN. THIS DATA IS FOR THE HIT WHICH PRODUCES INITIAL PLASTIC DEFORMATION

	$\chi = 2$–$\chi = 4$	$\chi = 4$–$\chi = 6$	$\chi = 6$–$\chi = 8$	$\chi = 8$–$\chi = 10$	$\chi = 10$–$\chi = 12$
			$\varepsilon = 85$ μin/in		
Δt (μ sec)	8·6	9·8	8·6	7·5	9·2
n	3	3	3	1	2
S.D. (μ sec)	1·8	1·0	1·4	—	1·0
			$\varepsilon = 131$ μin/in		
Δt (μ sec)	8·3	10·6	9·2	7·1	9·2
n	4	3	3	2	3
S.D. (μ sec)	2·1	2·1	1·8	0·5	1·2
			$\varepsilon = 170$ μin/in		
Δt (μ sec)	9·0	10·8	12·7	8·8	10·0
n	6	4	3	2	4
S.D. (μ sec)	3·3	3·1	5·9	0·5	3·3
			$\varepsilon = 213$ μin/in		
Δt (μ sec)	12·8	16·7	24·2	25·0	40·5
n	6	4	3	2	4
S.D. (μ sec)	4·3	6·3	26·0	10·0	58·4
			$\varepsilon = 255$ μin/in		
Δt (μ sec)	18·0	24·2	38·4	—	—
n	6	4	3	—	—
S.D. (μ sec)	5·8	7·5	25·0	—	—
			$\varepsilon = 298$ μin/in		
Δt (μ sec)	19·7	29·2	44·5	—	—
n	6	4	3	—	—
S.D. (μ sec)	5·6	8·7	19·6	—	—
			$\varepsilon = 340$ μin/in		
Δt (μ sec)	23·8	33·7	49·0	—	—
n	5	4	3	—	—
S.D. (μ sec)	4·6	10·2	24·1	—	—

The number of tubular specimens falling in 5 μsec intervals is shown in Figs. 9 and 10 for a strain of 213 μin/in. There is considerable difference in the nature of the distribution of times in Figs. 9 and 10. One of the main points of the present paper is the width of the distribution function as illustrated by Fig. 9 vis-a-vis the propagation time itself (approximately 20 μsec). More complete details are contained in Table 3, but typically the width of the distribution for strains near the yield point is twice the propagation time. A typical history near maximum strain is shown in Fig. 11 where the reflected wave is shown arriving at the various stations in sequence. At $\chi = 4$ in. the response is just what one expects. However there is a slowing down between $\chi = 4$ in. and $\chi = 6$ in. at large strains. The response between $\chi = 6$ in. and $\chi = 10$ in. is again quite normal.

Other data in which the specimen undergoes *very* small permanent strains on the first plastic hit are given later in the paper.

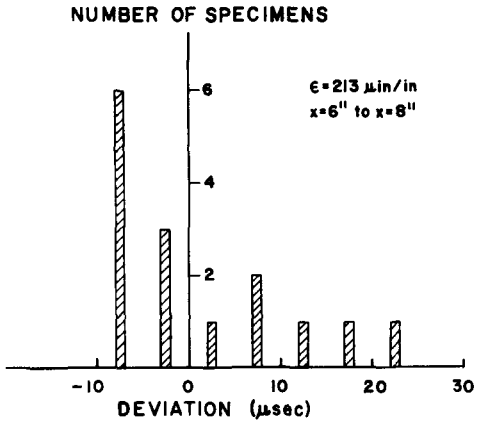

FIG. 10. The distribution of experimental values of the time required for a strain of 213 μin/in to propagate between $\chi = 6$ in. and $\chi = 8$ in. The number of specimens having a time interval which deviates from the average value of 14·8 μsec is given for 5 μsec intervals. All specimens are 0·50 in. o.d. tubes being subjected to stresses which here are producing the first permanent strains since being annealed.

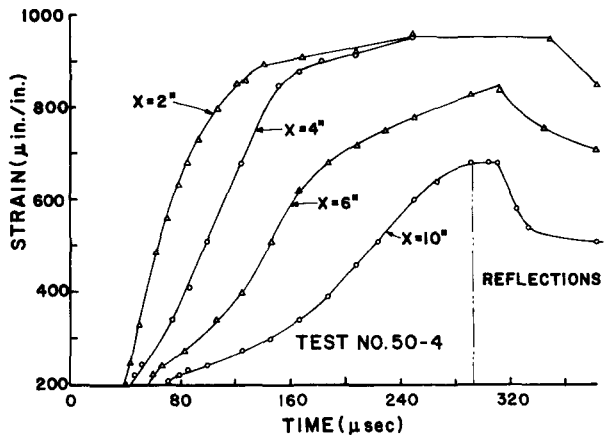

FIG. 11. A typical strain history of tubular specimens in the vicinity of the maximum strain produced by a small initial plastic impact. The specimen length is 35·8 in. and the permanent strains are (approximately): 700, 670, 550, 350, 300 μin/in at 2, 4, 6, 10 and 12 in. respectively.

First large hit

After several small plastic hits of the type just described, the spring is further compressed to produce a larger force at impact. It is of course expected that yielding will occur near the largest stress previously used and therefore there is little meaning to the value of the yield stress in these tests. Therefore the point of interest is the behavior of the wave at larger strains.

A typical example of these hits is shown in Fig. 12. As indicated in Fig. 12, the stations at $\chi = 12$ in. undergo less permanent strain than the positions closer to the impact face. Data such as that contained in Fig. 12 provide the increments in time for the wave to propagate between successive gauge positions. These times are then averaged as in the smaller elastic hits. The results are shown in Fig. 13 and Table 5. The major point of interest here

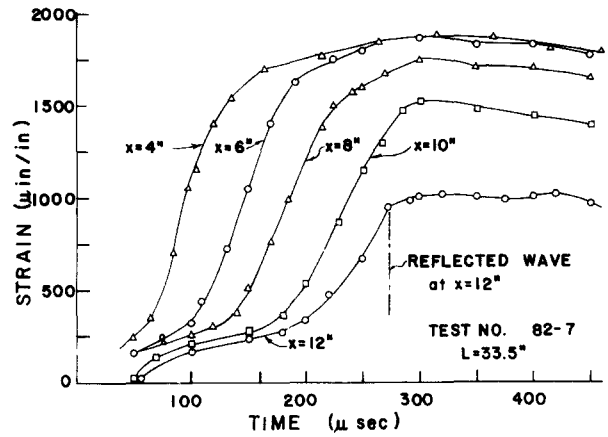

FIG. 12. A typical response at several axial positions for the first large plastic impact. The accumulated previous plastic strain is (approximately): 310, 220, 170, 60 and 35 μin/in at $\chi = 4$, 6, 8, 10 and 12 in. respectively; while the increments produced by this hit are 1680, 1530, 1340 and 850 μin/in at $\chi = 6$, 8, 10 and 12 in. respectively.

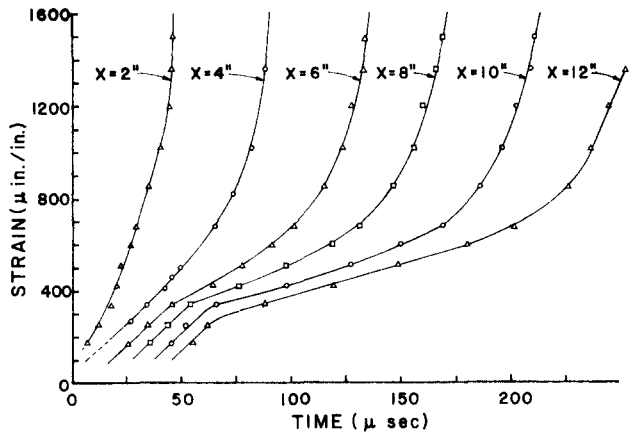

FIG. 13. The "averaged" strain histories at several axial positions for 0·50 in. o.d. tubular specimens subjected to stresses producing (relatively) large residual strains. The specimens had variable small amounts of plastic deformation prior to these particular hits.

is that for strains above 500 μin/in, the transit times are reasonably uniform. The distribution of sixty time increments for a strain of 595 μin/in is shown in Fig. 14. As before, this is a wide spectrum relative to the time increment itself. Figure 15 is the distribution of time increments for a strain of 680 μin/in propagating between $\chi = 4$ in. and $\chi = 6$ in. Figure 16 shows the distribution of sixty-six data points for strains of 850 μin/in. From Table 5 this strain clearly propagates at a constant speed. By comparing Figs. 9 and 15 one finds that the width of the distribution of the time increments in the large plastic strain region is much less than it is near the yield point. As indicated in Table 5, there still is more deviation between $\chi = 6$ in. and $\chi = 8$ in. than between the other stations. Figure 16 is taken as conclusive evidence, that the 3 μsec accuracy claimed above for the system is valid at larger strains, since even in this figure there is some real scatter in the material response.

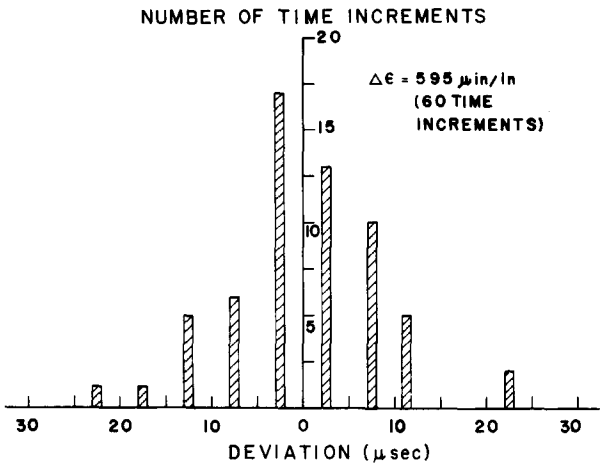

FIG. 14. The distribution of the experimental data on the time interval required for a change in strain of 595 μin/in to propagate two inches in hits like those shown in Fig. 12. The number of specimens having a time interval which deviates from the average value of 33·5 μsec is given for 5 μsec intervals.

TABLE 5. THE TIME INTERVAL, Δt, FOR A GIVEN VALUE OF THE CHANGE IN STRAIN, ε, TO PROPAGATE BETWEEN THE DESIGNATED AXIAL STATIONS IN 0·50-in. TUBULAR SPECIMENS OF ANNEALED ALUMINUM. THIS DATA IS FOR THE FIRST HIT WHICH PRODUCES LARGE PLASTIC DEFORMATIONS. MOST OF THE SPECIMENS HAD BEEN SUBJECTED TO PREVIOUS IMPACTS WHICH PRODUCED VARYING AMOUNTS OF PERMANENT STRAIN. THE NUMBER OF SPECIMENS, n; THE STANDARD DEVIATION, S.D.; THE MAXIMUM POSITIVE AND NEGATIVE DEVIATIONS IN THE TIME INTERVAL ARE ALSO GIVEN

	$\chi = 2$–$\chi = 4$	$\chi = 4$–$\chi = 6$	$\chi = 6$–$\chi = 8$	$\chi = 8$–$\chi = 10$	$\chi = 10$–$\chi = 12$
			$\varepsilon = 85$ μin/in		
Δt (μ sec)	—	10·2	9·3	11·4	10·6
n	—	5	8	10	3
S.D. (μ sec)	—	3·3	1·3	2·8	2·4
max. pos. dev. (μ sec)	—	6·6	2·5	6·7	3·0
max. neg. dev. (μ sec)	—	1·0	1·7	3·9	3·0
			$\varepsilon = 170$ μin/in		
Δt (μ sec)	8·2	10·5	9·2	10·2	10·2
n	6	14	14	13	5
S.D. (μ sec)	2·0	2·3	1·8	2·4	3·6
max. pos. dev. (μ sec)	3·5	6·2	3·3	6·1	6·5
max. neg. dev. (μ sec)	2·3	3·0	4·2	2·3	4·3
			$\varepsilon = 255$ μin/in		
Δt (μ sec)	10·5	14·6	10·4	16·2	22·4
n	9	17	13	15	9
S.D. (μ sec)	5·7	6·1	5·6	13·7	17·9
max. pos. dev. (μ sec)	10·3	14·5	12·1	38·8	34·6
max. neg. dev. (μ sec)	10·5	7·2	5·5	16·2	22·0
			$\varepsilon = 340$ μin/in		
Δt (μ sec)	14·3	19·0	17·1	21·5	29·5
n	10	21	17	18	9
S.D. (μ sec)	6·8	9·4	13·7	12·2	11·9
max. pos. dev. (μ sec)	13·9	16·8	26·2	15·2	20·5
max. neg. dev. (μ sec)	8·5	15·8	15·5	18·2	18·6

Table 5 (contd.)

	$\chi = 2$–$\chi = 4$	$\chi = 4$–$\chi = 6$	$\chi = 6$–$\chi = 8$	$\chi = 8$–$\chi = 10$	$\chi = 10$–$\chi = 12$
			$\varepsilon = 425$ μin/in		
Δt (μ sec)	23·5	26·0	21·0	29·5	30·3
n	10	20	17	20	9
S.D. (μ sec)	7·0	10·9	12·9	17·1	7·8
max. pos. dev. (μ sec)	9·8	20·2	22·9	53·4	6·3
max. neg. dev. (μ sec)	15·2	18·9	18·8	20·3	13·7
			$\varepsilon = 510$ μin/in		
Δt (μ sec)	29·5	29·7	27·4	31·8	27·9
n	10	21	18	18	8
S.D. (μ sec)	6·5	9·3	9·9	9·5	8·0
max. pos. dev. (μ sec)	7·3	21·9	15·3	11·5	12·2
max. neg. dev. (μ sec)	14·3	19·7	13·8	19·3	11·2
			$\varepsilon = 595$ μin/in		
Δt (μ sec)	33·2	34·1	33·1	34·1	33·0
n	10	21	18	16	6
S.D. (μ sec)	4·5	8·3	7·5	5·4	5·0
max. pos. dev. (μ sec)	5·9	18·3	17·0	7·5	8·7
max. neg. dev. (μ sec)	7·4	21·7	13·9	11·2	5·5
S.D. (neglecting 2 worst, μ sec)	3·7	5·4	6·4	4·4	2·5
			$\varepsilon = 680$ μin/in		
Δt (μ sec)	36·2	37·5	34·6	38·0	34·2
n	10	21	18	15	5
S.D. (μ sec)	3·3	5·7	7·8	3·9	4·3
max. pos. dev. (μ sec)	4·6	17·7	17·2	8·7	4·2
max. neg. dev. (μ sec)	4·6	9·0	11·2	8·8	6·7
			$\varepsilon = 850$ μin/in		
Δt (μ sec)	39·0	39·6	34·2	40·8	37·5
n	9	20	18	14	5
S.D. (μ sec)	3·4	4·8	8·3	3·7	4·8
max. pos. dev. (μ sec)	5·2	9·1	17·5	6·0	6·7
max. neg. dev. (μ sec)	6·5	9·3	14·2	6·8	6·7
			$\varepsilon = 1020$ μin/in		
Δt (μ sec)	41·3	41·7	39·8	43·8	37·3
n	10	20	16	13	4
S.D. (μ sec)	3·7	4·3	10·8	6·9	4·0
max. pos. dev. (μ sec)	6·3	7·5	21·0	17·2	4·3
max. neg. dev. (μ sec)	7·1	7·5	19·8	8·8	6·5
			$\varepsilon = 1360$ μin/in		
Δt (μ sec)	42·7	44·7	43·4	44·5	40·0
n	9	18	14	9	2
S.D. (μ sec)	4·1	4·8	12·7	5·3	1·0
max. pos. dev. (μ sec)	8·9	12·3	33·3	14·2	1·0
max. neg. dev. (μ sec)	6·1	11·4	14·2	8·8	1·0

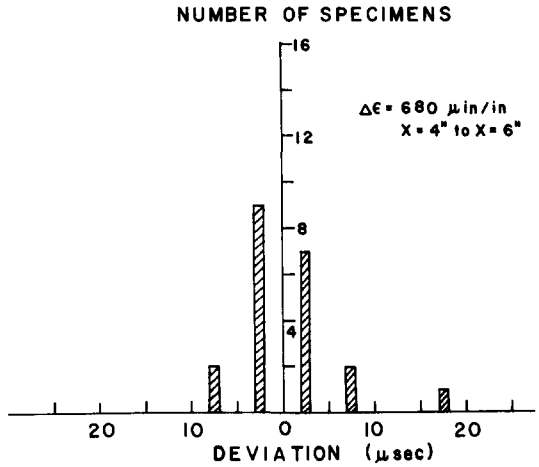

FIG. 15. The distribution of the experimental data on the time interval required for a change in strain of 680 μin/in to propagate between 4 in. and 6 in. in hits like Fig. 12. The number of specimens having a time interval which deviates from the average value of 37·5 μsec is given for each 5 μsec interval.

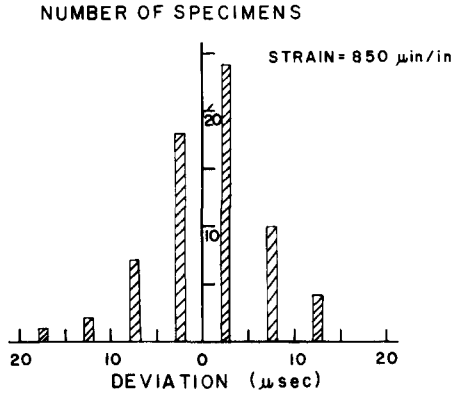

FIG. 16. The distribution of the experimental data on the time interval required for a change in strain of 850 μin/in to propagate 2 in. in hits like those shown in Fig. 12. The number of specimens having a time interval which deviates from the average value of 38·3 μsec is given for by 5 μsec intervals.

Very small plastic strains

Other interesting data are obtained during tests where the intention is to produce an elastic wave, but where the spring is inadvertently compressed a bit too much. Typical results are shown in Figs. 17–19. In Fig. 17, definite plastic strains existed after the test at $\chi = 4$ in. while $\chi = 12$ in. was perfectly elastic in its response. The gauge at $\chi = 8$ in. indicated some plastic strains after the test, but the value was within the variation due to other causes. However, if one uses a stress–strain relation where the tangent modulus continuously decreases, there is ample time for the plastic wave to propagate to $\chi = 12$ in. That is, it would only be a few percent slower than the elastic one. It is noted that the existence of a point of material instability near 150 μin/in in a static test of annealed aluminum is reported in [8]. Test No. 80-4, reported as Fig. 18, is very similar, except that the small, slowly

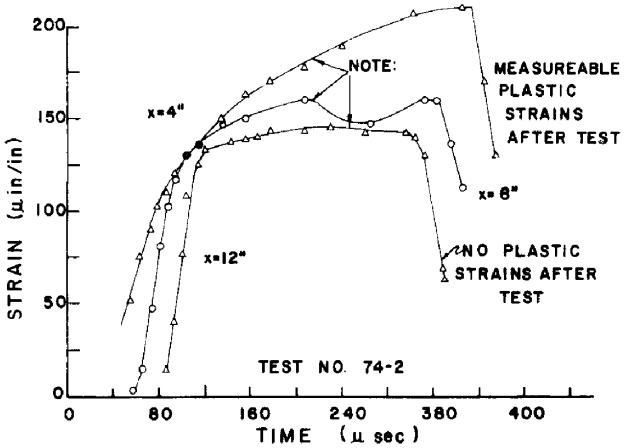

FIG. 17. Strain histories at several axial stations in a 0·50 in. o.d. tube in which the gauge at $\chi = 4$ in. undergoes a plastic strain while $\chi = 12$ in. remains elastic.

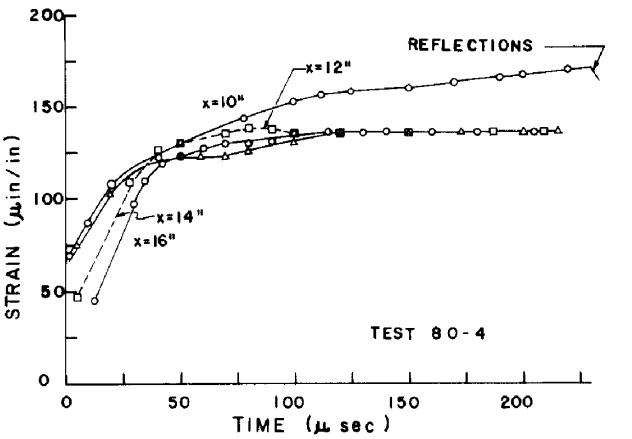

FIG. 18. Strain histories at several axial locations in a 0·50 in. o.d. tube in which the hit was intended to cause only elastic strains. However the point $\chi = 10$ in. is here seen to strain more than the others and also has a residual strain of 45 μin/in after the test.

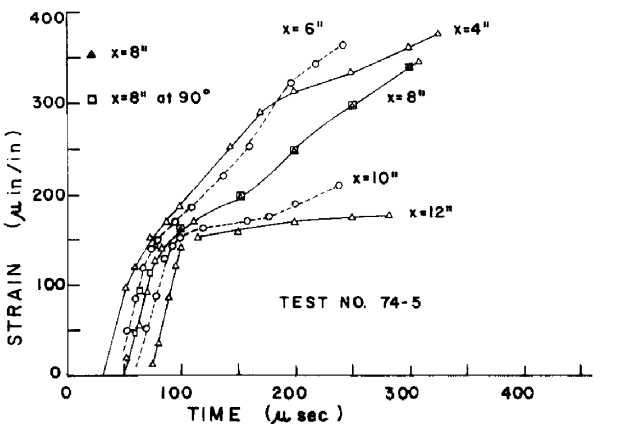

FIG. 19. Strain histories at several axial locations (two gauges at $\chi = 8$ in.) in a 0·50 in. o.d. tube in which $\chi = 12$ in. remains elastic while the others have permanent changes. The permanent changes are: 240, 270, 180, 85 and 0 μin/in at $\chi = 4$, 6, 8, 10 and 12 in. respectively.

propagating wave, is observed farther down the bar. In both Figs. 17 and 18, one observes deviations from the elementary picture of a bar which are similar to those found in the elastic range.

The largest impact in which $\chi = 12$ in. barely undergoes a plastic deformation is shown as Fig. 19. The rapidly decelerating wave is very clear at a strain of 175 μin/in. It is noted that this is the same specimen as shown in Fig. 17 and that is why the point $\chi = 4$ in. responds as it does. The final permanent strain in Fig. 19 is 100 μin/in at $\chi = 8$ in. while the record indicates 5 μin/in at $\chi = 12$ in. The latter value is not very reliable due to sensitivity and drift in the method of measurement. There are several examples where the reflected wave arrives at $\chi = 12$ in. before the oncoming plastic one. That is Fig. 19 is typical and not a unique one except for the size of strains at the forward gauges.

Other data

Figure 19 also contains a typical example of the "good" bending response as it includes the histories of two gauges located at the same axial station; but where one is located ninety degrees around the tube from the other. One cannot distinguish the difference between their responses at the scale used in Fig. 19 which demonstrates that there is very little bending in this test. In most tests, some bending could be observed at a more sensitive scale, but it is generally small. One can usually tell by the elastic response whether there will be appreciable bending in the plastic hits or not. This is considered to mean that, lack of initial specimen straightness is a prime cause of large bending in a properly aligned test.

This series of experiments was actually started to study the strain history at a given station; in order to observe if possible, whether or not a "shock wave" developed which would result in a jump in strain at a given gauge. This was not observed. The most interesting evidence in this direction was found in a 0·25 in. o.d. × 0·1875 in. i.d. tube in an exploratory type test; the response is shown in Fig. 20. It is possibly relevant that these specimens do not have quite the same metallurgical properties as the larger tubes and rods. In this specimen, a distinct plateau develops near 200 μin/in of strain and lasts for 160 μsec when the strain rate at $\chi = 12$ in. increases rapidly. When the strain-rate increases rapidly, the

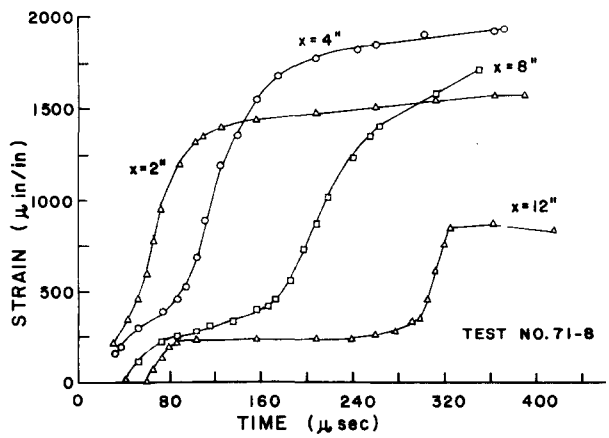

FIG. 20. Strain histories at several axial stations in a 0·25 in. o.d. tube showing an example of larger strains propagating faster than smaller ones, especially between $\chi = 8$ in. and $\chi = 12$ in.

propagation time required for the larger strains (say 500 μin/in) to propagate between $\chi = 8$ and $\chi = 12$ in. is less than it is for smaller values (say 250 μin/in). One can possibly interpret this as the initial phase of the formation of a "shock wave" near the position $\chi = 12$ in.

Typical strain histories of tests which used 90° rosette gauges to measure hoop strain as well as the axial component are shown in Figs. 21 and 22. These experiments were made in order to provide data on the deviation from the one dimensional state of stress assumed for the bar. As in the other tests, there is considerable variation in these data. The one invariant is the ratio of hoop to axial strains which remains *after* the test was over. This ratio is always between 0·48 and 0·50, consistent with the idea that plastic deformations are nearly incompressible. This is true for large or small residual strains.

The strain histories shown in Figs. 21 and 22, have a ratio of hoop to axial strains somewhat less than the 0·50. In Fig. 21, the ratio is approximately 0·42 for times prior to the

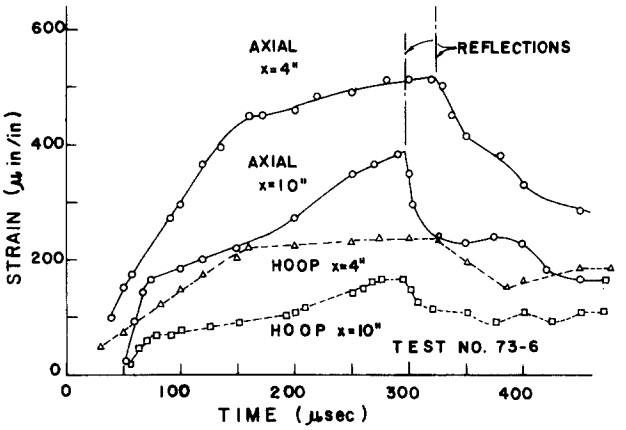

FIG. 21. Typical hoop and axial strain histories at two axial stations in a 0·50 in. o.d. tube. This specimen has no previous plastic deformation.

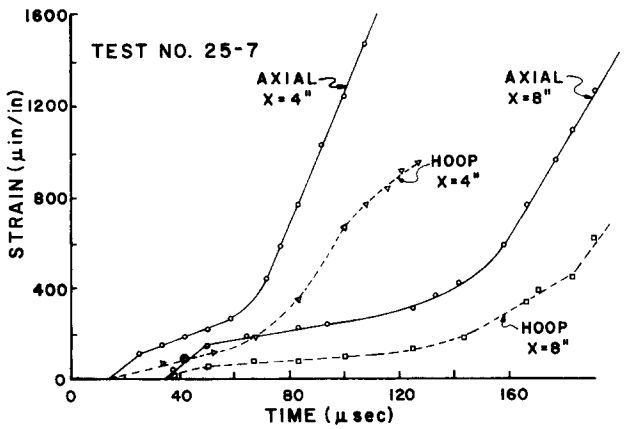

FIG. 22. Typical hoop and axial strain histories at two axial stations in a 0·50 in. o.d. tube for the (relatively) large impacts. This specimen had previously been deformed so that $\chi = 4$ in. had undergone about 1100 μin/in permanent strain and $\chi = 8$ in. had been deformed by 900 μin/in.

arrival of the reflected wave while the ratio is nearly 0·50 at $\chi = 4$ in. in Fig. 22. Perhaps the most important data, however, is the interval between 160 μsec and 320 μsec in Fig. 21 for the position $\chi = 4$ in. During this time the ratio of the *increment* in hoop strain to the *increment* of the axial strain is only 0·24. Therefore it seems clear that there are three dimensional (radial oscillations) effects which modify the elementary bar state of stress. However, these are not severe enough to invalidate certain other conclusions based on "averaged" data. In the elastic range, the ratio of maximum hoop to maximum axial strain is between 0·35 and 0·40; more frequently near the latter, indicating some three dimensional effects exist there as well.

When the unloading wave arrives at the interface, there is a separation of the specimen and plunger. There remains in the specimen however, a small amplitude wave which continues to propagate to and fro. When the impact is an elastic one, the amplitude of this wave is about 55 μin/in. When the impact is a plastic one, the amplitude is initially much larger than this and in fact, separation may not occur on the first reflection. By initially biasing the Ellis Associates Amplifier, it is possible to use exactly the same oscilloscope settings for observing this small wave in both the elastic and plastic ranges of the response. A schematic of the observations in a plastic impact is shown as an insert in Fig. 23. Also shown in Fig. 23 are typical results for the elastic, small plastic and large plastic impacts. At

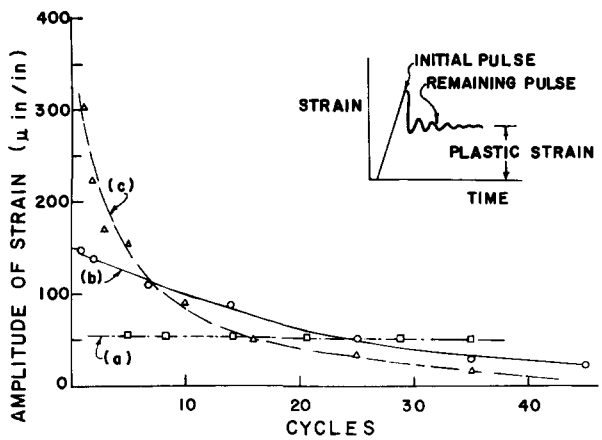

FIG. 23. A typical history of the decay in the amplitude of the strain increment that remains in the specimen after the plunger and specimen have separated (and therefore unloaded). Curves (a), (b) and (c) are for hits producing elastic, small plastic and large plastic strains, respectively.

the settings used, no measureable decay is found after 35 cycles in a hit where the amplitude of the pulse remaining is 55 μin/in in an elastic impact. However, in a hit which produces plastic deformation in part of the bar (due to reflections it is only in part), the wave is more rapidly attenuated and in fact is reduced well *below* 55 μin/in after 35 cycles, even though it is initially much greater. Figure 23 indicates a different damping mechanism for the very small strains, when plastic deformations exist and is possibly interesting from a metallurgical viewpoint.

The permanent strains that are produced in these specimens have a variation which is much less than we have reported above for the wave speeds. For example ten specimens were subjected to identical initial impacts which produced an average permanent strain of

1740 μin/in at $\chi = 4$ in. The standard deviation for these data is only 81 μin/in, a value which is only 4·5 percent. To the author this reinforces, from a different viewpoint, that the averaged stress–strain curve for these specimens is about the same. However the different specimens have a wider variety of the tangents to these curves than in the relations themselves. Figure 24 illustrates representative spatial variations in the permanent strain distribution for small, moderate and large initial impacts which produce plastic deformations. There is nearly uniform distribution in Fig. 24 for the first six inches.

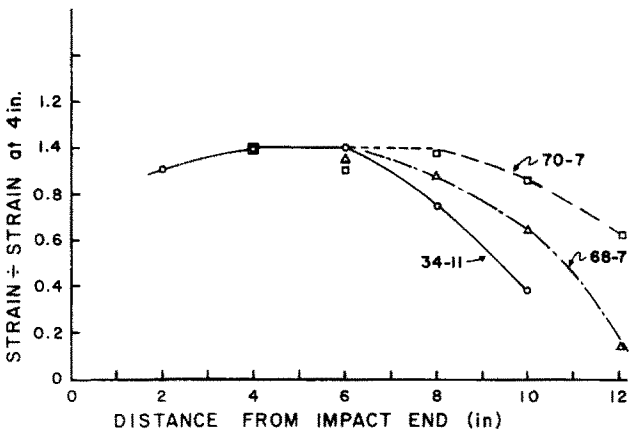

FIG. 24. Typical spatial variation of the permanent strain. The values are nondimensionalized by the strain at $\chi = 4$ in. which are: 610, 355 and 1620 μin/in for specimen no. 34–11, 68–7 and 70–7 respectively. All of these are the first impact which produces permanent strains.

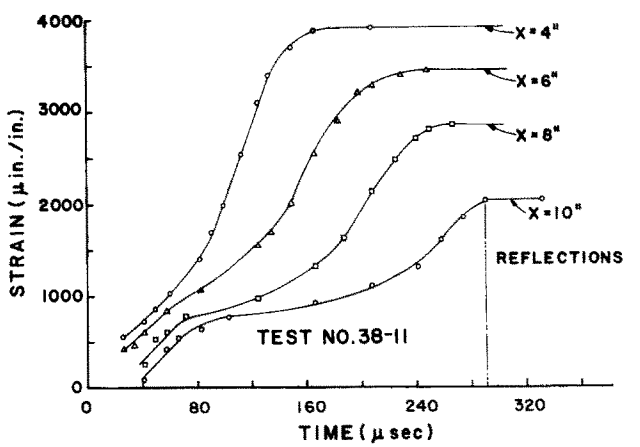

FIG. 25. A typical strain histories at several axial stations for the second large plastic impact. The total plastic strains prior to this impact are approximately: 3800, 3800, 3600, 3150 and 2750 μin/in at $\chi = 2$, 4, 6, 8 and 10 in. respectively. The plastic strain increments produced by this impact are: 2320, 2170, 1940, 1600 and 1130 μin/in at the same locations.

Hits after the first large plastic impact show the same variation in their details that the others do, and because of initial nonhomogeneity are even more difficult to interpret. Figure 25 however, is a response which is typical of many tests which produce large plastic deformations. It is the results of a second large impact at the settings used in producing first impacts

like Fig. 12. The permanent strains produced by the previous impacts of this specimen are: 1350, 1400, 1200, 925, and 670 μin/in during the small plastic hits and 2500, 2500, 2400, 2200, 2050 μin/in during the first large plastic hit at $\chi = 2, 4, 6, 8$ and 10 in. respectively. The significant feature of Fig. 25 is the *discreteness* of the maximum and permanent strains. Note in particular that the responses at $\chi = 4$ in., $\chi = 6$ in. and probably at $\chi = 8$ in., are flat *prior* to the arrival of a reflected wave at each position. The fact that the gauges at $\chi = 6$ and $\chi = 8$ in. do not continue to strain until they reach (or exceed) the response at $\chi = 4$ in. is believed to be related to a combination of three dimensional effects and unstable material response. Discussion of this point is delayed to the next section except to note that data like that in Figs. 11 and 12 is what one expects in Fig. 25 if the material is stable.

DISCUSSION AND INTERPRETATION

General

The data presented above is experimental data which is intended to be either as typical or as abnormal as possible, and to be relatively free of interpretation. The major point which it is believed the data given above has established is that the dynamic response of annealed aluminum in the plastic range is such that there is a real variation in propagation speed which is very large. Specifically, some individual specimens exhibit a response in which the propagation time between gauges is as much as double the average value, while others take nearly zero (see Fig. 2 and Table 3) time to propagate two inches. In this sense, Figs. 9 and 10 are regarded as typical. A second major point which the data establishes is that the response in the vicinity of yielding has an appreciably larger relative variation in propagation speed than it does at larger plastic strains. It is considered that a comparison of Figs. 9 and 10 with Fig. 15 proves this point.

The major cause of this wide spread in the propagation speed near yielding is the variation of the yield strain itself for specimens thought to be identical. Static test results [7] also have a deviation in them and the dynamic response being more or less related to the tangent of the stress–strain curve is even more sensitive to variations in the specimen properties. It is considered that the data in Table 3 suffices to demonstrate that above 500 μin/in the average speed of propagation is constant with distance down the bar (within the interval 2–12 in.) and therefore large amplitude waves are as adequately described by the strain-rate independent theory as by any other known to the author. This conclusion agrees with that reached by Bell [5, 6] several years ago. The strain-rates in the present study are about one percent of those involved in [5, 6] and more importantly, the maximum strains are much less than used by Bell. Furthermore we do not attempt measurements near the impact face and thereby we avoid the region where changes in the structure of the wave are severe. All of these contribute to making strain gauges appear to be adequate sensing devices. In addition we compare responses of identical systems, so that some errors of an absolute value are bypassed. Our system has the distinct advantage of making simultaneous measurements on the same specimen rather than on many as is done in [5, 6].

Dynamic yield strain

When one has very small hits so that some stations remain elastic while others go plastic, it is easy to define and measure a value of a "dynamic yield strain" which separates the elastic and plastic regions of the response. When plateaus are observed, as in Figs. 17 and 18, one also finds that the stations having a plateau suffer no permanent strain. Thus the

value of the plateau is also the "dynamic yield strain". Problems arise when every point undergoes plastic straining; but we are inclined to believe that an equivalent definition would be to use the value of the strain where the propagation speed becomes less than the elastic value.

In the analysis of the experimental data, there is still a lack of precision to the above statement. We use the propagation speed between $\chi = 4$ in. and $\chi = 10$ in. to establish a dynamic yield strain, since many specimens do not have any gauges at either 2 in. or 12 in. Furthermore, data from elastic impacts between these stations gave reasonably good agreement with the bar velocity. The response of three typical specimens, illustrating the variety of responses in individual tests, are shown in Fig. 26. Most specimens had responses like those labeled ① and ② in Fig. 26. That is where the propagation speed is constant

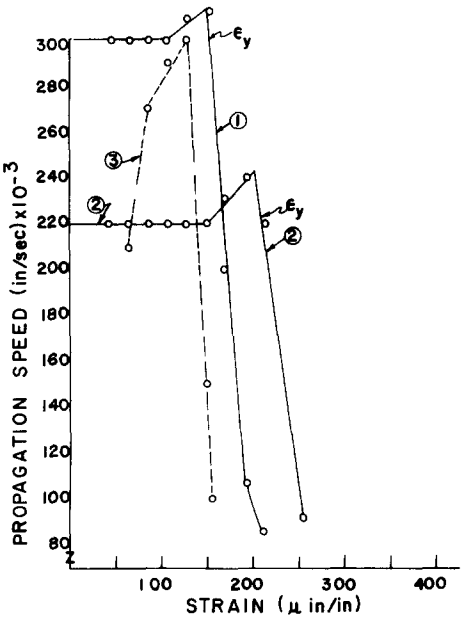

FIG. 26. Typical propagation speeds between gauges at $\chi = 4$ in. and $\chi = 10$ in. as a function of the strain for the first impacts producing permanent strain. Curves labeled ① and ② are typical of most specimens The dynamic yield strain is taken to be the point labeled ε_y on the on curve ②.

for a region, increases slightly* and then falls rapidly. Since there is the slight speeding up in Fig. 19, it was decided to use the strain on the falling side of Fig. 26, at the value where the speed equalled that of elastic region as the "dynamic yield strain". These are indicated as ε_y in Fig. 26. A few specimens responsed like curve ③ in Fig. 26, in which cases the strain at maximum speed is (arbitrarily) used as the "dynamic yield strain". Thus we establish experimental values of the "dynamic yield strain", for the entire group of 31 specimens which had gauges at $\chi = 4$ in. and $\chi = 10$ in. The average value and standard deviation of the "dynamic yield strain" are 173 μin/in and 33 μin/in respectively. In this 31 specimen sample the maximum and minimum "dynamic yield strain" is 232 and 110 μin/in, respectively. The

* This speeding up may be due to a change in the relative percentages of hydrostatic and deviatoric deformations in the actual state. This would be some basis for using the point where speeding up begins as a measure of the dynamic yield strain.

number of specimens falling within 10 μin/in intervals from the average of 173 μin/in are shown in Fig. 27. It is noted that the data in Table 3 is already appreciably slowed down to a speed of 137×10^3 in/sec at a strain of 170 μin/in. Thus the average of the yield points does not correspond to the yielding of the average response due to a difference in the nature of the averaging involved.

In the author's opinion, failure to consider the variation represented by Fig. 27 is at the heart of many of the discrepancies in the conclusions drawn by various investigators in the area of plastic wave propagation. It may be that the spread in our data is somewhat wider than in other studies, but it is believed to be a real fact of life that specimens have a wide variation in their response, and that dynamic tests are more sensitive to these than static results.

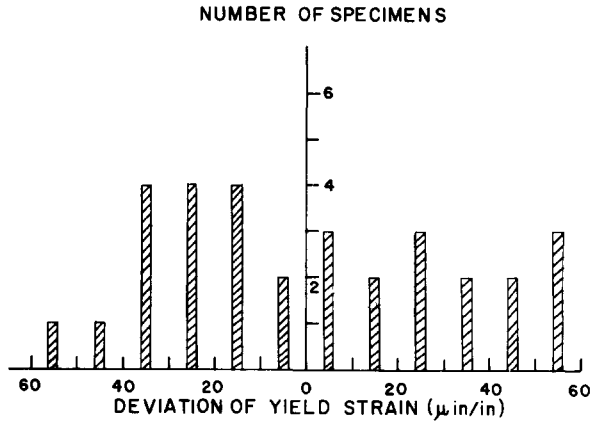

FIG. 27. The distribution of experimental values of the dynamic yield strain (ε_y of Fig. 26). The number of specimens in each 10 μin/in interval from the average of 173 μin/in are shown.

A derived stress–strain relation

One likes to compare the stress–strain relation obtained in static tests with that which applies to the dynamic problem. Under the assumption that the material is in fact strain-rate independent* this is easy to do. Either the Karman–Taylor–Rakhmatulin approach or the method of characteristics yield a stress–strain relation

$$\sigma = \int_0^{\varepsilon} \rho c^2 \, de \tag{1}$$

in which $c^2(\varepsilon)$ is regarded as the experimentally observed wave speed function and ρ is the mass density of the material. The data in Table 3 should be used directly for this calculation. However within the elastic region, the speed is slightly greater than the bar velocity (202×10^3 in/sec) and is presumably due to the same thing that causes the speeding up in Fig. 26. The data in Table 3 therefore yields (if used) a modulus greater than $10{\cdot}5 \times 10^6$ psi. To avoid this high modulus, the elastic region is therefore forced to travel at the bar velocity (see also Table 5) in this stress–strain calculation. The data for locations from $\chi = 4$ in. to

* A strain-rate effect means the inclusion of $\dot{\varepsilon}$ in the constitutive relation, *not* the observation that one gets a different stress–strain curve by moving the crosshead of the testing machine at different speeds. A material with a strain rate independent effect is one where stress σ is related to the strain ε by a relation of the type $\sigma = \hat{\sigma}(\varepsilon)$ and a strain-rate $\dot{\varepsilon}$ dependent material is one where the relation is of the form $\sigma = \bar{\sigma}(\varepsilon, \dot{\varepsilon})$.

$\chi = 10$ in. in Table 3 are used to construct a $c(\varepsilon)$ curve similar to those shown in Fig. 26. The bar velocity intersects this curve on the decreasing side at 135 μin/in. The data in Table 3 is then used in equation (1) to produce the plastic part of the stress–strain relation. The result is shown in Fig. 28 where it is compared with data from two static tests on the same material. The variation of the derived relation from the static curves is certainly within normal [3, 7] scatter for such data. It is noted that this agreement happens even though the data do not quite meet the test of having a constant speed of propagation.

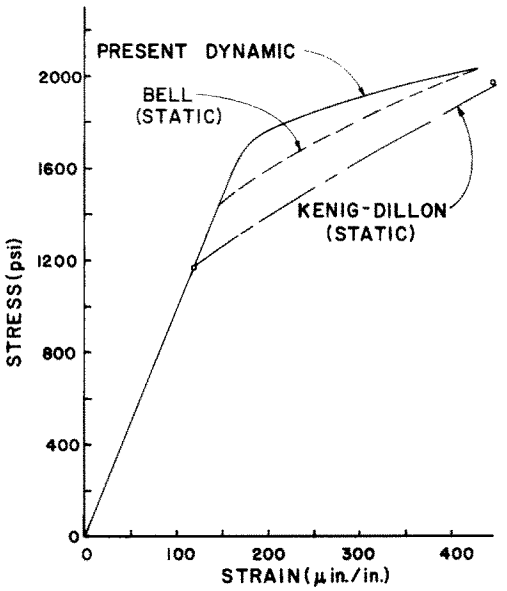

FIG. 28. The comparison of static and dynamic stress–strain relations. The dynamic curve is derived from the data between $\chi = 4$ in. and $\chi = 10$ in. in Table 3 and equation (1). The slope in the elastic region is forced to be equal to Young's modulus.

Unstable material data

The author has recently considered [2–4] annealed aluminum to be a mechanically unstable solid and illustrated some aspects of wave propagation in such substances. By an unstable material one means, that a small change in stress (say 3 psi) causes a large change in strain (say 200 μin/in) at certain discrete stresses while neighbouring values of the load cause nearly elastic changes in strain (say a 3 psi change in stress causing 0·5 μin/in change in strain). In particular it has been shown that certain properties of deformation waves which are sometimes attributed to strain-rate effects in the constitutive equation are also consistent with the unstable material concept and therefore may still be strain-rate independent. The serrated stress–strain relation has the advantage that one uses the same constitutive relation for slowly loaded tests and for impact studies. The only experimental fact* known to the author which is at variance with the unstable concept being applicable to annealed aluminum is the absence of a sudden jump in strain at a given axial station (see Fig. 15 of [2]) as predicted by using the serrated relation. One shows by the analysis of a

* This is really not a disturbing fact because the theory used is a shock approach utilizing "jump" conditions and the method of characteristics. By analogy with gas dynamics, one would expect to include heat conduction to study the "structure" of the shocks. Alternatively, strain-rate effects may enter at discrete stresses and be important in the structure of the wave in this sense.

boundary value problem that in unstable materials, due to "slow waves", the force on the end of the specimen depends on how fast the crosshead moves. Furthermore the strain is not uniform and therefore crosshead position is not a reliable measure of strain in such materials.

In order to avoid controversy, it is recalled [2] that the speed of propagation of most of a *large amplitude* wave is nearly the same for the material considered as being stable or unstable. The difference between stable and unstable materials is greatest in incremental situations. Clearly waves produced by incremental stresses can propagate at the bar velocity in the unstable material but will travel at a much lesser value in the stable one. The unstable concept is in much better agreement [8] with the experimental observations. Furthermore, there is Fig. 25, where the initial plastic deformation at $\chi = 4$ in. which is caused by previous impacts, exceeds those produced at $\chi = 6$ in. One therefore expects, if the material is stable and strain-rate independent, one of two things to happen. First, both positions could continue straining with time; or secondly, if the gauge at $\chi = 4$ in. reaches a plateau, the associated stress should propagate to the point $\chi = 6$ in. where it would be expected to cause the response to *exceed* the strain at $\chi = 4$ in. by the amount of the initial inhomogeneity. An example of this expected case is in fact given in Fig. 20. The fact that the gauge at $\chi = 4$ in. in Fig. 25 is constant for so long, as well as the slowing down of the response at $\chi = 6$ in. is taken to mean that conceivably (i.e. likely) a "slow" wave is propagating between $\chi = 4$ in. and $\chi = 6$ in. On the assumption that the unloading wave has not arrived at $\chi = 8$ in. during the time shown, the evidence then suggests another slow wave between $\chi = 6$ in. and $\chi = 8$ in. The gauge at $\chi = 10$ in. definitely sees an unloading wave at 285 μsec.

It appears to the author to be clearly established by the data shown in Figs. 17 and 19 that "proper" experimental technique gets a plastic deformation wave started along the specimen and that this disturbance then propagates* as a "slow" wave. That is at a propagation speed which is much less than the strain-rate independent theory of Karman, Taylor and Rakhmatulin or that in Fig. 7. The main feature of the experimental technique *is simply to attempt* to observe slow waves by hitting the specimen at a stress slightly above the yield point or by locating gauges farther down the bar, which we have not done. Using shock wave techniques one can show [2] by the analysis of unstable materials that one *must* do this type test in order to observe "slow" waves. Otherwise one excites a deformation which is a mixture of slow and fast waves which in turn propagates at a speed insensitive to the local material response curve. That is to say, at a speed which cannot be distinguished from the value given by the Karman–Taylor–Rahkmatulin theory with a smooth stress–strain curve. In particular one does not expect to see slow waves between $\chi = 2$ in. and $\chi = 4$ in. in unstable materials with an impact force as large as that used in Figs. 4–7. A comparison of Fig. 7 with Figs. 17 and 19 proves to us that there is ample time for the plastic wave to reach $\chi = 12$ in. before any reflected waves arrive there if the material is mechanically stable.

At first sight the data in Table 3 would be interpreted as proof that the response is that of a viscoelastic or viscoplastic (strain-rate sensitive) material. By curve fitting this can be made as reasonable as any other judgement *if this is all one knows about the material.* It is noted that the data are somewhat biased because specimens in which $\chi = 10$ in. or $\chi = 12$ in.

* Clearly these are not flukes which are attributable to strain gauge response. They always happen such that the deformation propagates through successive gauges. They are completely consistent with considerable data of a different type [4, 7]. Responses something like one of these figures are found *every* time one attempts to produce a very small plastic impact. That is the response in such attempts are either elastic or like one of these.

remain elastic are ignored, since averaging them with the others seems unreasonable. It is very clear that in the vicinity of the "yield stress", annealed aluminum is either: (a) viscoelastic or viscoplastic (b) unstable or (c) both. None of the solutions of strain-rate sensitive problems known [say 13, 14] to the author precisely cover the present boundary-value situation. However none of them even hints at phenomena like that shown in Fig. 19. The strain-rate near yielding at $\chi = 4$ in. in Fig. 7 is 4·5 μin/in/μsec while it is 1·9 in Fig. 19. Thus any "smooth" description of the response which applies would necessarily have a very high sensitivity to strain-rate in this region and therefore is likely to be inconsistent at larger strains. Furthermore tests in the direction of slightly higher strain-rates such as shown in Fig. 6, do not indicate high sensitivity to strain-rate. Considering the variety of results already [2, 4, 7] unified by the unstable material concept and the additional data presented here (Figs. 17, 19, 20, 25), as well as the nonexistence of explicit strain-rate results which apply qualitatively, the author concludes that it is appropriate to regard annealed aluminum as mechanically unstable. This is not inconsistent with using other descriptions of annealed aluminum in problems of limited range, provided one gains simplicity by doing so. In particular it is consistent with annealed aluminum being strain-rate independent in tests like those used in [5, 6], and represented here by tests given in Table 5.

CONCLUSIONS

1. The dynamic response of annealed aluminum in the plastic range is such that there is a real, large, variation in the propagation speed.
2. The variation in the response is (relatively) largest near yielding.
3. At strains above 500 μin/in the speed of propagation is constant along the bar in large impacts and therefore for large amplitude waves the material is as adequately described by the strain-rate independent theory as by any other.
4. The small amplitude pulse which remains in the specimen after unloading, attenuates very much more rapidly when plastic deformation has taken place than when the entire response is elastic. (See Fig. 23).
5. Additional data (i.e. Figs. 17–19) consistent with the concept that annealed aluminum is an unstable solid, but which none the less is possibly strain-rate independent in its response is presented. The variety of responses unified by the unstable concept make it desirable to first consider annealed aluminum as an unstable solid and to approximate to this according to the particular problem being considered. (Figs. 17–20, 25 of this paper as well as [2, 4, 7, 8]).

Acknowledgements—The author wishes to acknowledge the financial support of this research by the Air Force Office of Scientific Research by means of contract No. AF49(638)—1646. The assistance of B. Taylor, R. Siegfried, E. Klopp, D. Weaver and M. Miller in conducting the experiments and building the apparatus is very much appreciated. Many discussions with Professor J. Bell over several years are also acknowledged. It is hoped that the support given his work by an independent set of measurements will be useful to him. The assistance of Miss J. Hinkle in preparing the manuscript is also appreciated.

REFERENCES

[1] *Behavior of Materials Under Dynamic Loading*, edited by N. J. HUFFINGTON, JR. The American Society of Mechanical Engineers (1965).
[2] O. W. DILLON, JR., Waves in bars of mechanically unstable materials. *J. appl. Mech.* **33**, 267 (1966).
[3] O. W. DILLON, JR., Experimental data on aluminum as a mechanically unstable solid. *J. Mech. Phys. Solids* **11**, 289 (1963).
[4] M. J. KENIG and O. W. DILLON, JR., Shock waves produced by small stress increments in annealed aluminum. *J. appl. Mech.* **33**, 907 (1966).

[5] J. F. BELL, Propagation of large amplitude waves in annealed aluminum. *J. appl. Phys.* **31**, 277 (1960).
[6] J. F. BELL, Study of initial conditions in constant velocity impact. *J. appl. Phys.* **31**, 2188 (1960).
[7] MARVIN JERRY KENIG, Experiments on annealed aluminum. Ph.D. dissertation, Princeton University (1965).
[8] J. F. BELL and A. STEIN, The incremental loading wave in a pre-stressed plastic field. *Jnl Méc.* **1**, 395 (1962).
[9] W. N. SHARPE, JR., The Portevin–Le Chatelier effect in annealed aluminum. *J. Mech. Phys. Solids* **14**, 187 (1966).
[10] A. ROSEN and S. R. BODNER, The influence of strain rate and strain ageing on the flow stress of commercially pure aluminum. *Scientific Report No. 1*, Contract AF61(052)–951, Israel Institute of Technology (1966).
[11] RALPH PAPRINO and GEORGE GERARD, Dynamic stress–strain phenomena and plastic wave propagation in metals. *Trans. Am. Soc. Metals* **53**, 381 (1961).
[12] J. SPERAZZA, Propagation of large amplitude waves in pure lead. *Proc. 4th U.S. Natn. Congr. Appl. Mech.* p. 1123 (1962).
[13] W. E. BAKER and C. H. YEW, Strain rate effects in the propagation of torsional plastic waves. *J. appl. Mech.* **33**, 917 (1966).
[14] L. E. MALVERN, Experimental studies of strain-rate effects and plastic-wave propagation in annealed aluminimum. See [1].

(*Received* 17 *April* 1967; *revised* 27 *July* 1967)

Абстракт—Приводится эксшкриментальные результаты распространения волны деформации в отжигаемых алюминиевых трубах и стержнях, в которых максимальная осевая деформация находится между 100 μ дюйм/дюйм и 3000 μ дюйм/дюйм. Наблюдается большие изменение скорости распространения между образцами, которые считалось одинаковыми. Это изменение является действительным и релятивно большим в близи предела текучести, чем при больших величинах деформации. Для этого усредняются истории деформации, полученных на некотором числе образцев, чтобы было возможным сравнить многозначительные результаты с теоретическими результатами. Включается также стандардное отклонение результатов, используемое для получения скорости распространения. Оказывается, что в усредненной истории деформации свыше 500 μ дюйм/дюйм распространяются с постоянной скоростью и поэтому они согласны с теорией независимой от скорости деформации, как и с иной теорией. В усредненной истории деформации меньше 300 μ дюйм/дюйм обладают такой скоростью деформации, которая уменьшается при прохождении волны вдоль стержня и для этого влияет на очевидный эффект скорости деформации. Этот очевмдный эффект скорости деформации может касаться действительного или механически неустойчивого материала. Пьиводится результат, который строго подчеркивает, что неустойчивый материал является более обще применимым.